

Yoctosecond photon pulses from quark-gluon plasmas

Andreas Ipp,^{*} Christoph H. Keitel, and Jörg Evers[†]

Max Planck Institute for Nuclear Physics, Saupfercheckweg 1, D-69117 Heidelberg, Germany

(Dated: April 29, 2009)

Present ultra-fast laser optics is at the frontier between atto- and zeptosecond photon pulses, giving rise to unprecedented applications. We show that high-energetic photon pulses down to the yoctosecond timescale can be produced in heavy ion collisions. We focus on the high-energy photons produced during the initial phase of the expanding quark-gluon plasma. We study how the time evolution and properties of the plasma may influence the duration and shape of the photon pulse. Prospects for achieving double peak structures suitable for pump-probe experiments at the yoctosecond timescale are discussed.

PACS numbers: 25.75.Cj, 42.65.Re, 12.38.Mh, 78.47.J-

Recent advances in ultrafast laser optics aim at the creation of ultra-short pulses beyond the visible spectral range. Shorter pulses are desirable, since they provide better temporal resolution, while higher photon energy gives rise to better spatial resolution. High-order harmonics of femtosecond laser radiation have been shown to be sources of trains of attosecond XUV pulses [1, 2] that can be used to produce single attosecond X-ray pulses [3, 4]. For example, such single attosecond X-ray bursts [5] have applications in molecular imaging [6, 7, 8, 9, 10, 11], quantum control [12, 13], or Raman spectroscopy [14]. By introducing a controlled delay between two such peaks, the dynamics of electron systems could be studied using pump-probe techniques [4]. In view of the obvious desire for even shorter pulses with higher photon energies, it is reasonable to search for alternative production methods. In this spirit, it has been suggested that zeptosecond pulses could be created by focusing intense laser pulses on subwavelength-size structures [15], by the reflection of a relativistically intense femtosecond laser pulse from the oscillating boundary of an overdense plasma [16], or via nonlinear Thomson backscattering [17].

Among the shortest possible time scales that are available experimentally are those obtained through high-energy collisions. Particularly interesting in this context are heavy ion collisions that can produce a quark-gluon plasma (QGP), because they expose a complex system with rich internal dynamics that lives on a very short timescale. Heavy-ion collisions at RHIC and soon at the LHC produce this new state of matter up to the size of a nucleus (~ 15 fm) for a duration of a few tens of yoctoseconds ($1 \text{ ys} = 10^{-24} \text{ s} \approx 0.3 \text{ fm}/c$). In such a collision, the plasma is produced initially in a very anisotropic state, and reaches a hydrodynamic evolution through internal interactions only after some thermalization time τ_{therm} and isotropization time τ_{iso} . The observed particle spectra turned out to agree well with ideal hydrodynamical model predictions [18, 19, 20], which led to the assumption that the QGP thermalizes quickly, with isotropization times as low as $\tau_{\text{iso}} \approx 2 \text{ ys}$ ($0.3 \text{ fm}/c$). However, it

has been pointed out recently that viscous hydrodynamic models are still consistent with RHIC data if isotropization times as large as $\tau_{\text{iso}} \approx 7 \text{ ys}$ ($2 \text{ fm}/c$) are assumed [21], even if the expansion before isotropization is assumed to be collisionless (“free streaming”). Besides a plethora of particles that are created in such collisions, also high-energetic photons are produced and detected experimentally [22, 23, 24]. There are various mechanisms that lead to the production of photons in such a collision. Accordingly, these photons can be classified into direct photons, fragmentation photons, or background photons [25, 26]. It has been suggested that the isotropization time τ_{iso} can be measured using the direct photon yield [27, 28].

In this Letter, we study the production of high-energetic ultra-short photon pulses in the QGP. Direct photons produced in the spatially and temporally confined QGP are emitted on the yoctosecond timescale and are produced in the GeV energy range. We demonstrate that the emission envelope depends strongly on the internal dynamics of the QGP. Under certain conditions, a double peak structure in the emission envelope can be observed, which could be the first source for pump-probe experiments at the yoctosecond timescale. We find that the delay between the peaks is directly related to the isotropization time, and the relative height between the peaks can be shaped by varying photon energy and emission angle. Such pulses could be utilized, for example, to resolve dynamics on the nuclear timescale such as that of baryon resonances [29]. As an alternative interpretation of our results, a time-resolved study of the emitted photons could provide a window to the internal QGP dynamics throughout its expansion.

Our analysis can be outlined as follows. The QGP is formed in a collision of two heavy ions as illustrated in Fig. 1(a-c), and we study the emission of direct photons from the expanding extended QGP. The energy spectrum of such photons extends to the GeV range, and the upper limit for the temporal duration of the GeV photon pulse is given by the expansion dynamics of the QGP, which leads to yoctosecond pulses. Regarding the shape of the pho-

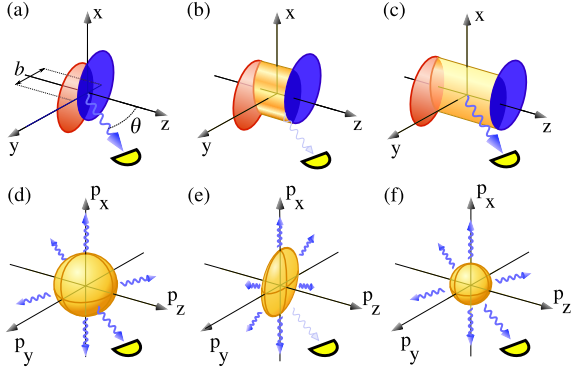


Figure 1: (Color online) Different stages in the high-energy collision. (a)-(c) show three snapshots in time in position space. Shown are the two relativistically contracted colliding ions that create the quark-gluon plasma in the overlap region. Curly arrows denote photon emission and semicircles the detectors. (d)-(f) are corresponding pictorial representations of the plasma in momentum space. In an intermediate stage, the momentum distribution is anisotropic, resulting in a change in the angular photon emission pattern that can give rise to double-peaked photon pulses.

ton pulse, we find that the angle-resolved photon emission rate strongly depends on the internal state of the plasma, characterized by the momentum distribution of the plasma constituents, see Fig. 1(d-f). For an intermediate time after the collision, a momentum anisotropy occurs, which leads to a preferential emission of the photons perpendicular to the beam axis z . A photon detector placed towards the beam axis would therefore measure a time-dependent photon flux depending on the time evolution of the plasma. Based on a recent model [30, 31] for the internal plasma dynamics, we find that this mechanism can give rise to double-peaked pulse envelopes that could be utilized for pump-probe experiments.

We base our model on the one-dimensional expansion model by Bjorken [32]. This assumes boost-invariant evolution of the quark-gluon plasma in a central region of the collision. The detector is placed away from the beam axis by an angle θ , and for a sufficiently far away detector, the light paths from the QGP to the detector are parallel. We restrict ourselves to the production of direct photons from the QGP, and will not consider other photon production mechanisms of the collision, since QGP photons capture well the dynamics of the collective evolution [24, 27]. The leading contribution to the photon production rate R originates from quark-gluon Compton scattering and quark-antiquark annihilation. Including a propagator resummation in the thermal, isotropic medium, it can be expressed in the following analytic way [33]

$$E \frac{d^3 R}{d^3 k} = \frac{5}{9} \frac{\alpha \alpha_s}{2\pi^2} T^2 e^{-E/T} \ln \left(\frac{2.912 E}{4\pi \alpha_s T} \right) \quad (1)$$

where α is the fine structure constant ($\hbar = c =$

$k_B = 1$ in the formulae), α_s the corresponding quantity for the strong force, E and k are the photon energy and momentum, and T the temperature of the medium. The anisotropy is described by a parameter $\xi = \langle p_T^2 \rangle / (2 \langle p_L^2 \rangle) - 1$ that relates the mean longitudinal and transverse momenta p_L and p_T . We use a recent model to describe the time evolution of the QGP [30, 31]. This model specifies the time evolution for the energy density $\mathcal{E} = \mathcal{E}(\tau)$, for the hard scale $p_{\text{hard}} = p_{\text{hard}}(\tau)$ (which corresponds to T in the isotropic case), and for the anisotropy parameter $\xi = \xi(\tau)$ as a function of the proper time τ . These quantities scale with different powers depending on the QGP expansion dynamics. For example, the time evolution of the anisotropy parameter can be written as $\xi(\tau) = (\tau/\tau_0)^\delta - 1$ with an exponent δ . In the free streaming phase, $\delta = 2$, while in the ideal hydrodynamic phase $\delta = 0$. Other scenarios lead to exponents between those two extreme cases, for example $\delta = 2/3$ for collisional broadening. The model in Ref. [31] essentially introduces a smeared step-function for the exponent $\delta = \delta(\tau)$ to interpolate between $\delta = 2$ (or $\delta = 2/3$) at early times $\tau \ll \tau_{\text{iso}}$ and $\delta = 0$ at late times $\tau \gg \tau_{\text{iso}}$, where the duration of the transition is controlled by τ_{iso}/γ with dimensionless parameter γ . In the model, thermalization and isotropization happen concurrently, $\tau_{\text{therm}} = \tau_{\text{iso}}$.

In the radial direction, we use a straightforward generalization of the temperature dependence $T(r, \tau_0) = T_0 [2(1 - r^2/R_T^2)]^{1/4}$ [34, 35] for non-central collisions that is valid in the overlap region of the colliding nuclei. As in Ref. [31], we neglect the expansion of the QGP into transverse directions, since it is small in the initial stage throughout which the high-energetic photons are emitted. T_0 is the initial temperature, r is the distance from the center in radial direction, and R_T is the transverse radius of the nucleus. The number of photons of frequency ω_d that arrive at the detector at time t_d in the laboratory system can be obtained by integrating the photon rate (1) along all possible light paths. The world-line of the photons that hit the detector at laboratory time t_d can then be parametrized as $\mathbf{z}(t; t_d, x_k, y_k) = x_k \hat{\mathbf{k}}_1^\perp + y_k \hat{\mathbf{k}}_2^\perp + \hat{\mathbf{k}}(t - t_d + d)$, where $\hat{\mathbf{k}}$ is the spatial direction of the light wave vector $k = (\omega, \mathbf{k})$, $\hat{\mathbf{k}}_1^\perp$ and $\hat{\mathbf{k}}_2^\perp$ are two direction vectors orthogonal to \mathbf{k} and to each other, and d is the distance to the detector. The transverse shift away from the origin is parametrized by x_k and y_k . The signal f_d that arrives at the detector at time t_d is given by integrating the photon emission rate along the photon world line $f_d(k, t_d, x_k, y_k) = \int_0^{t_d} dt f(k, t, \mathbf{z}(t; t_d, x_k, y_k))$ where $f(k, t, \mathbf{z})$ is the photon emission rate in the laboratory frame inside the QGP, and vanishing outside the plasma region. In order to calculate f_d , one needs to transform $f(k, \tau, 0) \equiv E d^3 R / (d^3 k)$ from the local rest frame into the laboratory system. Integrating over the displacement parameters x_k and y_k , one obtains the photon rate per unit time and frequency interval with A_d the

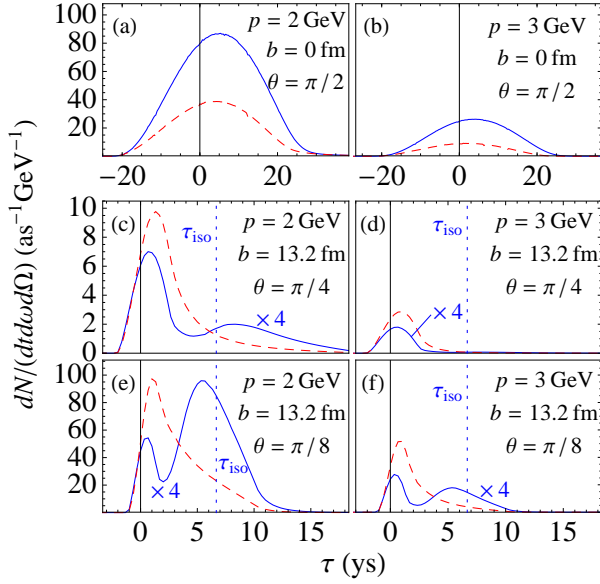


Figure 2: (Color online) Photon emission rate as a function of detector time τ . Solid blue lines show a large isotropization time $\tau_{\text{iso}} = 6.7 \text{ ys} = 2 \text{ fm}/c$ with $\delta = 2$ (free streaming model) while dashed red lines correspond to a short isotropization time $\tau_{\text{iso}} = \tau_0 = 0.3 \text{ ys} = 0.088 \text{ fm}/c$. The left [right] column shows emission with photon energy 2 GeV [3 GeV]. (a,b) display emission at midrapidity ($\theta = \pi/2$) for a central collision with impact parameter $b = 0$. (c-f) show double-peaked photon pulses obtained for $b = 13.2 \text{ fm}$, and the vertical dotted line indicates the position of the larger $\tau_{\text{iso}} = 6.7 \text{ ys}$. The solid blue lines are scaled by a factor of 4. In (c,d) the detector direction is $\theta = \pi/4$, in (e,f) it is $\theta = \pi/8$.

detector area,

$$\frac{d^2 N(\omega_d, t_d)}{dt_d d\omega_d} = \frac{A_d}{8\pi d^2} \int dx_k dy_k \omega_d f_d(\omega_d, t_d, x_k, y_k). \quad (2)$$

For the calculation we followed the parameters as given in [31]. We show results for LHC energies, where the initial conditions are given by a formation time $\tau_0 = 0.3 \text{ ys} (= 0.088 \text{ fm}/c)$, the initial temperature $T_0 = 845 \text{ MeV}$, and transverse radius of the lead ion $R_T = 7.1 \text{ fm}$. The critical temperature, where the QGP ceases to exist, is taken as $T_C = 160 \text{ MeV}$. Ref. [31] compared the two models free-streaming ($\delta = 2$) and collisional-broadening ($\delta = 2/3$) with parameter $\gamma = 2$. The isotropization time was varied in the range $\tau_{\text{iso}} = \tau_0$ or $\tau_{\text{iso}} = 6.7 \text{ ys} (= 2 \text{ fm}/c)$. Both possibilities are not yet ruled out by RHIC data. We use the model with fixed final multiplicity, where the initial conditions are adjusted as a function of τ_{iso} in order to result in the same final entropy as for $\tau_{\text{iso}} = \tau_0$.

Figures 2(a,b) show the typical time evolution of the photon emission rate for a central collision with emission angle orthogonal to the beam axis ($\theta = \pi/2$). The origin of the abscissa is the time when a photon emitted from the center of the collision arrives at the de-

tector. Photons arriving earlier originate from a part of the QGP that is closer to the detector. The pulse shape is mainly determined by the geometry of the nucleus with radius 7.1 fm . While the first photons arrive shortly after $-7.1 \text{ fm}/c = -24 \text{ ys}$, the final photons arrive later (up to 30 ys) due to the finite life-time of the plasma. As in Refs. [28], we observe an enhancement of the integrated photon yield with increasing isotropization time τ_{iso} . Corresponding plots for collisional broadening ($\delta = 2/3$) show the same trend, but less pronounced.

Internal QGP dynamics occur on a timescale of a few fm/c . Any structure of this order is washed out simply by the time for light to cross the size of the QGP. We apply two strategies to overcome this limit. First, we reduce the physical extent of the QGP by considering non-central collisions with impact parameter b . Second, an optimization of the detection angle minimizes the traveling time through the plasma. In forward direction, the initial shape of the QGP is Lorentz-contracted, hence light travels through the initial shape quickly. This is partially spoiled due to the QGP expansion in the same direction. Thus intermediate emission angles are most promising for which the QGP appears partly Lorentz contracted but does not expand towards the detector.

Figures 2(c-f) show the photon emission in a direction away from midrapidity $\theta \neq \pi/2$ for a non-central collision. The impact parameter $b = 13.2 \text{ fm}$ corresponds to an overlap region of the size $1 \text{ fm} \times 3.6 \text{ fm}$. Here, a striking new double-peak structure appears. Roughly speaking, the minimum between the peaks corresponds to the maximum of the anisotropy parameter $\xi(\tau)$, which grows with exponent $\delta = 2$ for $\tau < \tau_{\text{iso}}$, and vanishes for $\tau > \tau_{\text{iso}}$. This is because the photon emission rate is suppressed for larger values of ξ and smaller values of θ [27]. The distance between the two peaks is therefore approximately governed by τ_{iso} , indicated by the dotted line in Figs. 2(c-f).

The dynamics shown in Fig. 2 require a more detailed interpretation. Since the QGP is expanding in the longitudinal direction, photons produced in the receding tail arrive at the detector at later times. These photons are red-shifted in energy, whereas photons that are emitted in the approaching part of the QGP are blue-shifted. But not only the energy is shifted, also the time evolution is dilated through relativistic effects. This is manifested in a longer tail of the photon shape, compared to the same non-central collision at midrapidity. In Figs. 2(c-f), the first peak corresponds to photons emitted from the blue-shifted part of the QGP, while the second peak corresponds to photons emitted from a slightly red-shifted and time-dilated part of the plasma. For comparison, for a short isotropization time $\tau_{\text{iso}} = \tau_0$ (dashed lines) the separation into two peaks does not occur. Therefore this effect is very sensitive to the internal dynamics of the QGP.

The relative size of the first and second peak is con-

trolled both by the emission angle and by the photon energy. The first peak becomes larger at increasing emission angles mainly because the second peak is suppressed due to the geometry. The second peak is governed by photons emitted from the receding part of the plasma, but the phase space for such photons is constricted for larger emission angles. For smaller impact parameters or larger QGP sizes, the second peak overlaps with the first, thereby washing out this structure.

Our results are based on a number of model assumptions. For example, we did not take into account the transverse expansion, which would become important at later times. It could either enhance the double peak structure through a further separation of red- and blue-shifted parts of the QGP, or reduce the effect through a prolonged photon passage through the QGP. These modifications may cause qualitative changes to the photon emission envelope, but not to the yoctosecond timescale. Besides the photons produced in the QGP that we have calculated, in an actual experiment there is a background of photons from different sources [34]. These include photons produced by a jet passing through the QGP [35], and could dominate the effect that is expected from the QGP alone. Since these photons are produced on a similar yoctosecond timescale, they can be expected to have the positive effect of enhancing the photon rate of the pulse. But at the same time they would constitute a background for the pulse shape determination. Other background photons are produced at different time scales, e.g., due to decay of pions produced in the hadronization of the QGP.

We now turn to an estimate of the photon production rate. In the GeV energy range, these are of the order of a few photons per collision [34]. Note that a single GeV photon pulse of 10 ys duration corresponds to a pulse energy of only about 100 pJ, but to a power of 10 TW. Increasing the collision energy would further enhance the number of photons produced. A comparison of photon emission contributions of RHIC and LHC suggests that this would also increase the relative importance of the contribution of thermal photons compared to other kinds of photons [34].

Concluding, we have studied the time evolution of the photon emission from the QGP. Since the QGP only exists on the yoctosecond timescale, it naturally emits photons at this timescale. We have shown that the emission envelope can be influenced by the geometry, emission angle, and internal dynamics like the isotropization time of the expanding QGP. For a particular parameter range, that is non-central collisions, large isotropization time, and an emission angle close to forward direction, a double peak structure has been found within our model. If experimental problems could be overcome and a controllable photon emission shape could be obtained, this would open a new window for studying dynamics at the nuclear time scale. Pump-probe experiments at the GeV

energy scale could be envisioned. Experiments at this energy range are currently conducted via bremsstrahlung at synchrotrons [36], but so far these experiments do not allow for time-resolved studies. Alternatively, determining the photon emission shape experimentally would give direct access to dynamic properties of the QGP, like its isotropization time.

We thank K. Z. Hatsagortsyan and M. Strickland for helpful discussions.

* Electronic address: andreas.ipp@mpi-hd.mpg.de

† Electronic address: joerg.evers@mpi-hd.mpg.de

- [1] N. Papadogiannis *et al.*, Phys. Rev. Lett. **83**, 4289 (1999).
- [2] P. Paul *et al.*, Science **292**, 1689 (2001).
- [3] M. Hentschel *et al.*, Nature **414**, 509 (2001).
- [4] Y. Silberberg, Nature **414**, 494 (2001).
- [5] T. Baeva *et al.*, Laser Part. Beams **25**, 339 (2007).
- [6] J. Itatani *et al.*, Nature **432**, 867 (2004).
- [7] M. Lein *et al.*, Phys. Rev. A **66**, 023805 (2002).
- [8] H. Niikura *et al.*, Nature **417**, 917 (2002).
- [9] S. Baker *et al.*, Science **312**, 424 (2006).
- [10] M. Lein, Phys. Rev. Lett. **94**, 053004 (2005).
- [11] T. Ergler *et al.*, Phys. Rev. Lett. **97**, 193001 (2006).
- [12] H. Rabitz *et al.*, Science **288**, 824 (2000).
- [13] Y. Silberberg, Nature **430**, 624 (2004).
- [14] N. Dudovich, D. Oron, and Y. Silberberg, Nature **418**, 512 (2002).
- [15] A. E. Kaplan and P. L. Shkolnikov, Phys. Rev. Lett. **88**, 074801 (2002); W. R. Garrett, *ibid.* **89**, 279501 (2002); A. E. Kaplan and P. L. Shkolnikov, *ibid.* 279502 (2002); G. Stupakov and M. Zolotarev, *ibid.* 199501 (2002); A. E. Kaplan and P. L. Shkolnikov, *ibid.* 199502 (2002).
- [16] S. Gordienko *et al.*, Phys. Rev. Lett. **93**, 115002 (2004).
- [17] P. Lan *et al.*, Phys. Rev. E **72**, 066501 (2005).
- [18] P. Huovinen *et al.*, Phys. Lett. B **503**, 58 (2001).
- [19] T. Hirano and K. Tsuda, Phys. Rev. C **66**, 054905 (2002).
- [20] M. J. Tannenbaum, Rept. Prog. Phys. **69**, 2005 (2006).
- [21] M. Luzum and P. Romatschke, Phys. Rev. C **78**, 034915 (2008), 0804.4015.
- [22] J. Adams *et al.* (STAR), Phys. Rev. C **70**, 044902 (2004).
- [23] S. S. Adler *et al.* (PHENIX), Phys. Rev. Lett. **94**, 232301 (2005).
- [24] A. Ipp *et al.*, Phys. Lett. B **666**, 315 (2008).
- [25] K. Reygers, AIP Conf. Proc. **892**, 413 (2007).
- [26] S. Turbide, R. Rapp, and C. Gale, Phys. Rev. C **69**, 014903 (2004).
- [27] B. Schenke and M. Strickland, Phys. Rev. D **76**, 025023 (2007).
- [28] L. Bhattacharya and P. Roy, arXiv:0809.4596 [hep-ph].
- [29] M. Dugger *et al.*, Phys. Rev. C **76**, 025211 (2007).
- [30] M. Martinez and M. Strickland, Phys. Rev. Lett. **100**, 102301 (2008).
- [31] M. Martinez and M. Strickland, Phys. Rev. C **78**, 034917 (2008).
- [32] J. D. Bjorken, Phys. Rev. D **27**, 140 (1983).
- [33] J. I. Kapusta, P. Lichard, and D. Seibert, Phys. Rev. D **44**, 2774 (1991).
- [34] S. Turbide *et al.*, Phys. Rev. C **72**, 014906 (2005).
- [35] R. J. Fries, B. Müller, and D. K. Srivastava, Phys. Rev.

- Lett. **90**, 132301 (2003).
- [36] W. Chang, Few-body systems **41**, 95 (2007).